NILES

Journal of Laser Science and Applications
journal homepage: https://jlsa.journals.ekb.eg

Cairo University

Laser-Assisted Surface Treatment of Ti64 Alloy for Industrial Applications

Samar Reda Al-Sayed[1*] and Aliaa Abdelfatah[2]

[1] Department of Engineering Applications of Lasers, National Institute of Laser Enhanced Sciences, Cairo University, Egypt, [2] Corrosion and Surface Treatment Lab., Dept. of Metallurgy, Faculty of Engineering, Cairo University, Egypt

Abstract

Purpose: Ti-6Al-4V is one of the most frequently used titanium alloys in the field of industry owing to its outstanding properties that stem from its high strength-to-weight ratio, the unique combination of ease machinability, good biocompatibility, and corrosion resistance. Such alloy is commonly used in the manufacture of submarines and the petrochemical industries which is exposed to different corrosive media such as seawater. This present study seeks to increase the corrosion resistance of Ti64 alloy by means of laser surface treatment.

Methodology: Laser surface treatment has been accomplished by melting the Ti64 surfaces using ultra-short pulses from a Q-switched Nd: YAG laser. Laser fluence (F_L) with several values was utilized to accomplish the proper laser fluence which gives the optimal performance.

Results: After laser surface melting, the microstructure became more homogeneous with finer grain size, 2 µm for surfaces treated at 65 J.mm^{-2} vs. 145 µm for the untreated surfaces, this could be due to the quick self-quenching associated with the laser melting. The micro-hardness increased to a maximum of 500 $HV_{0.3}$ at 65 J.mm^{-2} due to the formation of needle-shaped martensite α` Ti phase subsequent to the rapid solidification.

The results revealed a reduction in the corrosion rate from 0.75 µm/Y for untreated titanium alloy to 0.07 µm/Year for the laser-treated alloys, consequently, it was confirmed that the laser fluence had a substantial impact on both surface hardness and corrosion resistance.

Conclusion: The laser surface melting using nanoscale pulses from a Q-switched laser system could be applied to successfully enhance the corrosion resistance and the surface hardness of Ti64 titanium alloys.

Keywords— laser melting, titanium alloy, corrosion resistance

I. Introduction

Titanium, dual-phase alloys have been categorized as the main production material in many engineering applications, specifically in the fields of industrial applications such as submarines and petrochemical industries [1, 2]. Such titanium alloys have poor wear resistance that limits their applications, in addition, the formation of a porous titanium oxide layer causes the loss of adhesion at the interface [3, 4]. The dense TiO_2 film formed on ultra-fine surfaces has improved bonding with the substrate, reducing the likelihood of film delamination or breakdown under aggressive environmental conditions. Recently, numerous surface modification technologies have been developed to improve the surface properties of such alloys [5]. To enhance the surface properties of this alloy, different traditional treatments were applied such as the solution and aging treatments however, these treatments lead to many disadvantages such as long and complex treatment procedures. On the other hand, when the laser beam is used as a source of heat most of those disadvantages are limited [6, 7]. Laser surface treatment was commonly used to enhance the mechanical performance and corrosion resistance of different ferrous and nonferrous alloys, however, few researchers have considered the surface properties after laser melting of titanium and its alloys [8]. Mishra et al. [9] investigate the effect of different laser powers on the microstructure and mechanical properties of α + β titanium alloy (VT31) for the aerospace industry, a significant improvement in the hardness values has been accomplished by laser treatment. Such an increase in the hardness values (up to 750 HV) was attributed to the transformation that occurred in the microstructure, and enrichment of β-phase existed in the laser-affected zone. Another research studied the influence of laser surface treatment of Ti-6Al-4V titanium alloy for bio-implant application [10], the authors investigate the corrosion resistance after laser treatment in a simulated body fluid. They reported that the corrosion potential increased and the primary potential for pit formation substantially as compared to the untreated Ti-6Al-4V surfaces. In Ohtsu et al. study [11], the hardness of titanium surfaces modified by laser beam irradiation at different wavelengths, 532 nm, and 1064 nm, they found that the craters' size and depth steeply increased with an increase in the laser beam power; at the same time, oxide layer thickness that surrounded the crater

Received 19th December 2024
Accepted 29th January 2025
Corresponding author: Samar Reda Al-Sayed Email: sreda@niles.edu.eg

increased as well. Moreover, many researches dealt with β-type titanium alloys, for example, the study of Y. Michiyama and K. Demizu [12] which proposed different age hardening speeds depending on the conditions of the solution treatment to investigate the wear resistance. Two heating methods were adopted, furnace heating and laser heating after furnace heating, the results revealed that the weight loss of the titanium alloy remarkably decreased with hardness especially that was above 450HV.

In this study, laser surface treatment of Ti64 titanium alloy was accomplished using nano pulses from a Q-switched Nd:YAG laser. Different laser fluences (F_L) were applied to get the optimum laser processing conditions that achieved better surface properties. The laser processing parameters have been chosen to avoid any micro-cracks formation on the laser-treated surfaces. Microstructure, micro-hardness, and corrosion resistance corresponding to each laser processing parameter have been investigated. The laser treatments (LT) were adopted to enhance the micro-hardness and the corrosion resistance performance of laser-treated Ti-6Al-4V titanium samples.

II- METHODOLOGY

2.1. Materials and laser experiments

Ti64 samples with dimensions of 30 mm×30 mm×0.5 mm was chosen as substrate. The substrate surfaces were cleaned using acetone before laser processing to remove any dirt and increase the laser absorptivity. The laser treatment was carried out using a Q-switched Nd:YAG laser with laser parameters listed in **table 1**. The schematic design of the laser treatment process is illustrated in **fig. 1**. Some preliminary experiments with several laser interaction times were conducted, starting with 10 minutes to 30 minutes with a step of 5 minutes, nevertheless, macro-cracks have been observed on the titanium surfaces, and consequently, smaller laser interaction times lower than 5 minutes have been selected. After such preliminary attempts range of laser fluences was identified to verify the optimum processing conditions for LT. Different laser fluence was calculated as listed in **table. 2** based on different laser interaction times using the following equations:

$$E_t = E_p * r * t \quad (1)$$

Where E_t is the total energy provided to the sample in Joule, *Ep* is energy per pulse in Joule, *r* is the frequency in Hz, and *t* is the exposure time in seconds.

$$F_L = E_t / A \quad (2)$$

Where F_L is the total laser fluence delivered to the sample in J.mm^{-2}, and *A* is the laser beam area in mm^2.

Table 1. Parameters of Q-switched Nd:YAG laser system

Laser parameter	Value
Max Energy	50 J
Energy/Pulse	0.0076 J
Frequency	10 Hz
Beam diameter	0.3 mm
Laser interaction time	60, 120, 180, 240

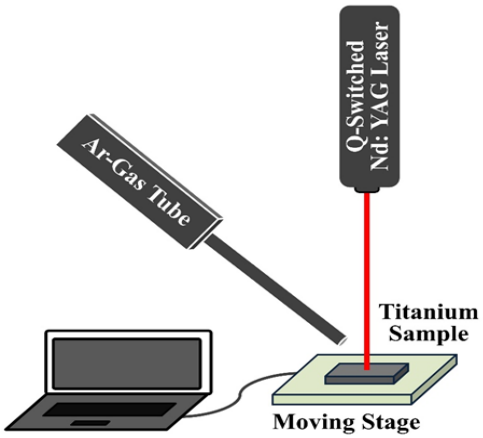

Figure 1. Schematic design of the laser treatment process.

Table 2. Laser fluence calculations

Laser interaction time (s)	Total energy (J)	Laser fluence (J.mm^{-2})
60	4.6	65 (F_{L1})
120	9.12	130 (F_{L2})
180	13.68	195 (F_{L3})
240	18.24	260 (F_{L4})

2.2. Morphological Characterization, Micro-hardness, and Electrochemical Measurements

Laser-treated samples were mounted, polished, and etched through the standard metallographic procedures to investigate the microstructural modifications through optical as well as scanning electron microscopes. Micro-hardness distributions were measured using an HMV digital micro-hardness tester, obtaining values in the Vickers scale. All surfaces were tested under a load of 0.5 N and a dwell time of 15 s. For each condition, an average value of 5 indentations was recorded.

The investigated samples were ground and polished before the corrosion test. The corrosion performance was examined in a corrosive medium of 0.6M NaCl. The Potentio-dynamic-polarization test was performed using three-electrode cells using PGZ 100 Potentio-stat with Volt. Lab 6 software. A saturated calomel electrode (SCE) was employed as the reference electrode and a platinum electrode was used as the auxiliary electrode. Every sample was subjected to the test conditions for 60 minutes to attain the steady-state open-circuit potential (OCP). The Potentio-dynamic tests were accomplished from – 0.5 V versus OCP to +0.5 V versus OCP and the corrosion currents were registered. The electrochemical parameters during the test usually include the corrosion potential (E_{corr}) and corrosion-current density (i_{corr}). The parameter, i_{corr}, can be used to calculate the average corrosion rates from equation (3) which represents the general corrosion resistance [13] :

$$Corrosion\ rate\ (mm/year) = 3.27 \times 10^{-3} \times i_{corr}\, \rho \times E_W \quad (3)$$

Where ρ is the density of the alloy in g.cm^{-3}, i_{corr} (in μA.cm^{-2}) is the corrosion current density, and E_W is the equivalent weight of the alloy in g.equiv^{-1}.

III- RESULTS AND DISCUSSION

3.1. Characteristics of the treated-layer and micro-hardness measurements

The Ti64 commercial alloy was received in the annealed condition. The annealed microstructure consists of (α + β) phases; equi-axed α with inter-granular β of a comparatively uniform grain size as shown in **fig. 2**.

Figure 2. Optical micrograph of the cross-section of Ti64

Scanning electron micrographs of the upper surface of samples processed at different laser fluences are illustrated in **fig. 3**, as can be seen from the micrographs all surfaces have homogenous structures with ultrafine grain size. The microstructure of the untreated Ti64 transformed from coarse grains microstructure to fine grains with a homogeneous microstructure accompanying laser treatment. The grain size was measured utilizing image software analysis through the SEM, and the grain size was noted to decrease as the laser fluence was reduced. The grain size measured around 2 µm and 4 µm for samples processed at 65 and 260 J, respectively, compared to the extremely coarser grain size of 150 µm for the untreated samples. Usually, the cooling rates associated with laser surface melting could range from 10^3 K/s to 10^6 K/s [14], depending on the laser processing parameters such as laser power, scanning speed, as well as material absorption. Such rapid cooling rates indicate a substantial undercooling, increasing nucleation within the molten pool while suppressing grain growth due to its limited time, which results in a refined grain structure [15]. Consequently, it could be confirmed that laser pulses from Q-switched Nd:YAG laser leads to a remarkably large refinement of grain structure and overcome the main problem of coarse grain size associated with the as-received structure of Ti64 titanium alloy [16].

In **fig. 4(a)**, the cross-sectional SEM micrographs show the entire treated layer which contains three different zones, the melting zone (MZ), the fusion zone (FZ), and the untreated surface. In the MZ, a large area of fine needle-like α` martensite phase is randomly distributed in the β grains, along with the β phase through the initial α phase due to the extremely high cooling rates. During the laser treatment process, the untreated bottom of the substrate provided a heat sink to lower the temperature of the molten pool allowing a faster solidification rate associated with the laser self-quenching, consequently, the steep temperature gradient from the melted layer was large, resulting in a speedy solidification process of the molten pool. As a consequence, the growth of the phase was prevented and a very hard martensite (α`) phase formed instead [11].

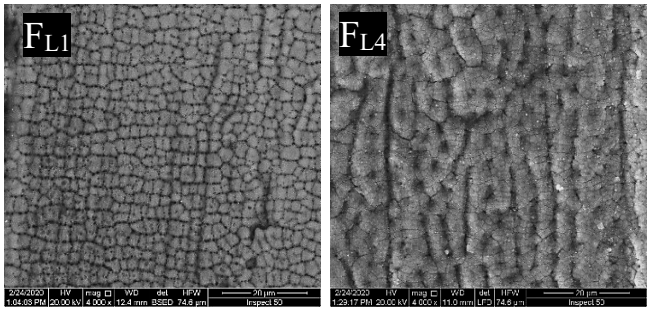

Figure 3. SEM of the upper surface of laser-treated samples processed at different laser fluences

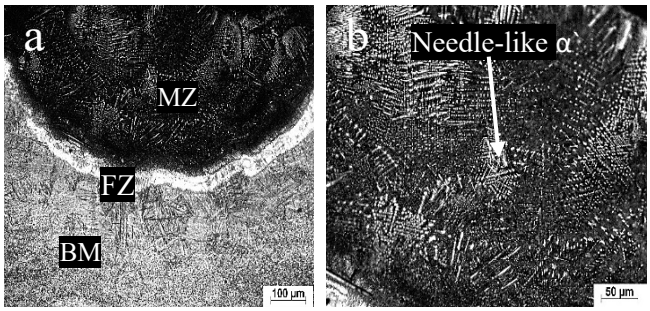

Figure 4. OM micrographs of the laser-treated Ti64 samples processed at 260 J.mm^{-2} (a) entire layer, (b) melting zone

In **fig. 5**, the micro-hardness values of the untreated titanium alloy and the treated ones for all laser processing conditions are exhibited. The micro-hardness of the untreated Ti64 samples is about 180 $HV_{0.3}$. On the other hand, the micro-hardness of the titanium surfaces after laser treatment is significantly increased, especially when the lowest laser fluence value was applied to the surface, the increase is near threefold the initial micro-hardness value.

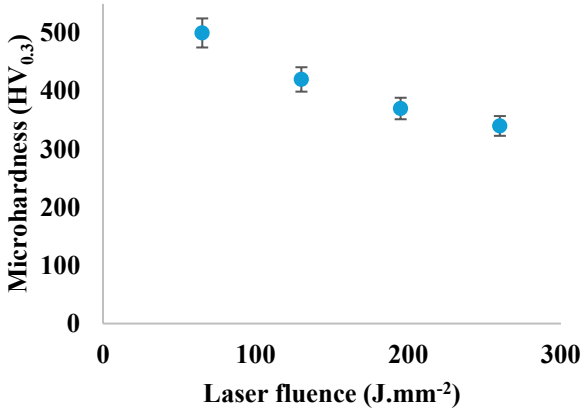

Figure 5. Micro-hardness of the laser-treated samples vs. laser fluence

Primarily as a result of the formation of a very hard needle-like martensite phase after laser treatment because the laser beam rapidly heats the surface to high temperatures even above the melting point followed by quick cooling.

During the heating and cooling cycles, the phase (β) transformed into the hard martensite phase (α`) which results in high hardness values. In addition, such severe quenching can lead to the formation of finer microstructure, and as normal the finer grain structure is harder due to the difficulty of dislocation movement along the grain boundaries [17]. Moreover, when the dislocation density increases also increases the strength offering more resistance to the material deformation which is reflected again in the hardness value. Finally, the residual stresses that form throughout the microstructure play a critical role in the determination of the resistance of the material to plastic deformations [6].

3.2. Electrochemical characterization

Potentio-dynamic polarization results of the laser-treated layers and the as-received in 0.6 wt. % NaCl solution at room temperature are presented in **fig. 6**. The untreated surfaces showed a corrosion rate of 0.75 µm/Y, contrary it is noticed that no considerable difference in the trend of the four polarization curves of the titanium surfaces after laser treatment, which reveals that the same reaction occurs on the titanium surface after laser treatment nevertheless at different corrosion rates as listed in **table. 2**.

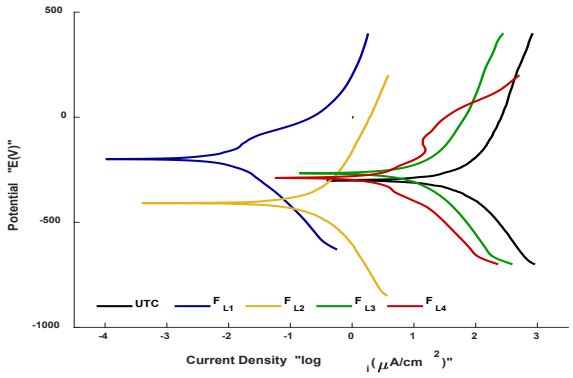

Figure 6. Tafel polarization curves for untreated surface a(UTS) and all laser conditions

As can be seen from the corrosion rates, the E_{corr} values for all laser-treated samples are nearly close, whereas the E_{corr} value for the untreated surfaces recorded a corrosion rate of 0.75 µm/Y, which is greater than the value of samples treated at FL_1 by 11 times. The rapid solidification as a result of partial surface melting caused the formation of a very fine microstructure with a high density of grain boundaries which weakens the surface corrosion resistance. Moreover, such refined grains provide a significant number of grain boundaries, which act as a diffusion pathway for oxygen through the oxidation process.

A considerable percentage of the precipitated salts on the treated surfaces were acquired on the treated titanium surfaces (utilizing EDX analysis). Furthermore, the laser-treated surfaces show dense TiO_2 film, as listed in Table 3. This may be attributed to the dependency of the underlying treated surfaces with ultra-fine microstructure which led to the inhibition of alloying elements micro-segregation [18]. Additionally, such uniform microstructure establishes a more compact and chemically stable passive layer compared to untreated titanium surfaces, which often have coarser grains and less homogeneous oxide films. Also, the TiO_2 film contained few defects/pores, which decreases pathways for corrosive agents to initiate localized corrosion. Such results imply that the stability of passive film formed on laser-treated samples at such specific laser conditions is better than that of the untreated titanium surfaces. Consequently, it could be concluded that the samples processed at a laser interaction time of 60 seconds are further favorable to enhancing the corrosion performance of such alloys. Excessively high laser fluence could lead to excessive oxidation, forming thicker and potentially less adherent oxide layers [19].

Table 3. Polarization corrosion parameters

Treatment conditions	Corrosion Rate (µm/Y)	$i_{corr.}$ (nA/cm²)
F_{L1}	0.07	0.125
F_{L2}	0.172	0.4
F_{L3}	0.2	107
F_{L4}	0.35	58

Table 4. Elemental EDX analysis of surfaces after corrosion test

Treatment conditions	Titanium (Ti)	Oxygen (O)	Other elements C, Na, Cl, Al, V
As received	76%	11%	13%
F_{L1}	41%	42%	17%

IV. Conclusions

An attempt was accomplished to enhance the surface properties of Ti64 alloy by applying a Q-switched laser for surface melting. A substantial refinement of microstructure and formation of needle-like martensite α` with a partial amount of β phase after the laser surface melting. In summary:

1. A maximum micro-hardness of 500 $HV_{0.3}$ of the laser-melted layer was reached as compared to the micro-hardness associated with the untreated substrate of 180 $HV_{0.3}$.
2. The untreated substrates possess a corrosion rate of 0.75 µm/Y, however corrosion rate after laser melting is decreased to 0.07 µm/Y at a laser fluence of 60 $J.mm^{-2}$. This could be attributed to the more stable TiO_2 film on the treated surfaces.
3. Finally, ultra-short pulses from a Q-switched laser considerably improve the corrosion resistance of Ti64 alloys at low laser fluence with a small laser interaction time.

References

1. S.R. Al-Sayed, H. Elgazzar, A. Nofal, Microstructure Evaluation and High-Temperature Wear

Performance, Metals and Materials International (2022). https://doi.org/https://doi.org/10.1007/s12540-021-01160-x.
2. S. Al-Sayed Ali, A. Hussein, A. Nofal, S. Hasseb Elnaby, H. Elgazzar, H. Sabour, Laser Powder Cladding of Ti-6Al-4V α/β Alloy, Materials 10 (2017) 1178. https://doi.org/10.3390/ma10101178.
3. A. Biswas, Laser Surface Treatment of Ti-6Al-4V for Bio-Implant Application, n.d. https://www.researchgate.net/publication/266186790.
4. S.R. Al-sayed, F.A. Samad, T. Mohamed, Novel Surface Topography and Micro-hardness Characterization of Laser Clad Layer on TC4 Titanium Alloy Using Laser-Induced Breakdown Spectroscopy and Machine Learning, Metallurgical and Materials Transactions A (n.d.). https://doi.org/10.1007/s11661-022-06772-5.
5. I. García, J.J. De Damborenea, Corrosion properties of TiN prepared by laser gas alloying of Ti and Ti6A14V, Corros Sci 40 (1998) 1411–1419. https://doi.org/10.1016/S0010-938X(98)00046-8.
6. S.R. Al-Sayed, A.A. Hussein, A.A. Nofal, S.I. Hassab Elnaby, H. Elgazzar, M.S. Steel, Characterization of a Laser Surface-Treated Martensitic Stainless Steel, Materials 10 (2017) 595. https://doi.org/10.3390/ma10060595.
7. S.R. Al-Sayed, H. Elgazzar, A. Nofal, A comparative study of laser fluence effect on surface modification and hardness profile of austempered ductile iron, Journal of Materials Research and Technology 31 (2024) 3189–3204. https://doi.org/10.1016/j.jmrt.2024.07.052.
8. C.L. Meléndez, J.G. Chacón, Corrosion Behavior of Ti-6Al-4V Alloys, 7 (2012) 2389–2402.
9. A.S. Chauhan, J.S. Jha, S. Telrandhe, S. V, A.A. Gokhale, S.K. Mishra, Laser surface treatment of α-β titanium alloy to develop a β -rich phase with very high hardness, J Mater Process Technol 288 (2021). https://doi.org/10.1016/j.jmatprotec.2020.116873.
10. A. Biswas, L. Li, T.K. Maity, U.K. Chatterjee, B.L. Mordike, I. Manna, J. Dutta Majumdar, Laser surface treatment of Ti-6Al-4V for bio-implant application, Lasers in Engineering 17 (2007) 59–73.
11. N. Ohtsu, M. Yamane, K. Kodama, K. Wagatsuma, Surface hardening of titanium by pulsed Nd:YAG laser irradiation at 1064- and 532-nm wavelengths in nitrogen atmosphere, Appl Surf Sci 257 (2010) 691–695. https://doi.org/10.1016/j.apsusc.2010.07.025.
12. Y. Michiyama, K. Demizu, Surface age hardening and wear properties of beta-type titanium alloy by laser surface solution treatment, Mater Trans 52 (2011) 714–718. https://doi.org/10.2320/matertrans.MBW201003.
13. A. Abdelfattah, L.Z. Mohamed, S. El-Hadad, M.E. Moussa, G.A. Gaber, Comprehensive investigation of Si additions and nanocomposite inhibitors on microstructure/ corrosion performance of cast AX53 alloy in 3.5% NaCl solution, Surface Review and Letters (2024). https://doi.org/10.1142/s0218625x25500507.
14. T.N. Baker, Laser Surface modification of Ti alloys, Woodhead, UK, 2010.
15. W. He, Y. Zhao, Q. Wei, H. Liu, D. Song, Z. Sun, Effect of cooling rates and Fe contents on microstructure evolution of Al-Cu-Mn-Mg-Fe-Si alloys, Mater Charact 214 (2024). https://doi.org/10.1016/j.matchar.2024.114074.
16. D.R. Tobergte, S. Curtis, Microstructure and Texture in Steels and other Materials, Springer-Verlag, India, 2008. https://doi.org/10.1017/CBO9781107415324.004.
17. S. Graça, R. Colaço, P.A. Carvalho, R. Vilar, Determination of dislocation density from hardness measurements in metals, Mater Lett 62 (2008) 3812–3814. https://doi.org/10.1016/j.matlet.2008.04.072.
18. F. Wang, D. Ma, A. Bührig-Polaczek, Microsegregation behavior of alloying elements in single-crystal nickel-based superalloys with emphasis on dendritic structure, Mater Charact 127 (2017) 311–316. https://doi.org/10.1016/j.matchar.2017.02.030.
19. X. Zhang, T. Chang, H. Chen, S. Wang, Y. Yang, S. Zhou, C. Liu, Z. Zhang, Optimizing laser parameters and exploring building direction dependence of corrosion behavior in NiTi alloys fabricated by laser powder bed fusion, Journal of Materials Research and Technology 33 (2024) 4023–4032. https://doi.org/10.1016/j.jmrt.2024.10.105.